The distribution of cellular turnover in the human body

Ron Sender and Ron Milo ✉

We integrated ubiquity, mass and lifespan of all major cell types to achieve a comprehensive quantitative description of cellular turnover. We found a total cellular mass turnover of 80 ± 20 grams per day, dominated by blood cells and gut epithelial cells. In terms of cell numbers, close to 90% of the $(0.33 \pm 0.02) \times 10^{12}$ cells per day turnover was blood cells.

To better understand the function of the human body in health and disease, it is of major interest to quantify its cellular composition and turnover. The most recent rigorous census[1–3] has estimated the number of cells in the adult body to be approximately $30 \pm 0.5 \times 10^{12}$, of which about 90% are from the hematopoietic lineage, mostly red blood cells (RBCs)[2,3]. Yet beyond this static view, there is no corresponding overall census of the dynamics of death and regeneration of cells and tissues.

Here we fill this knowledge gap concerning overall cellular turnover dynamics of the human body by surveying the variation in lifespan exhibited by different cell types and quantifying the cellular turnover rates in terms of both mass and number.

For our survey, we adopted the standard reference person, which was historically defined as a male 'between 20–30 years of age, weighing 70 kg and 170 cm in height'[4]. As the cell turnover rate may change due to different illnesses, we added the qualification 'healthy' to the standard reference. Cellular turnover rates, of course, vary among people based on their sex, age, state of health and many other factors. However, the scarcity of comprehensive data in the literature limits the ability to perform a similar holistic analysis for other population groups and remains to be conducted in future work that can follow the methodology presented here. Nonetheless, we do discuss major quantitative implications of variations in dominant factors contributing to our main results across sex, age and health status.

The lifespan of a cell varies greatly across cell type and tissue, from 3–5 d for gut epithelia, to years (and even a lifetime) for cardiomyocytes or neurons. We define the daily cellular turnover rate as the average daily number of cell deaths in a specific cell population. We note that continuous recycling of intracellular components, important for cellular maintenance and accounting for a large fraction of the overall energetic flux of the body, does not lead to cell death and is thus not a case of cellular turnover. In steady state, cell death and production rates average out, yielding a simple relation between the number of cells, n, of a given type, their mean lifespan of τ days, and the cellular turnover rate of β cells per day: $\beta = n/\tau$. The daily cellular turnover rate is affected by two factors: the number of cells and their mean lifespan (measured from their last division). Thus, a given cell population will contribute substantially to the overall cellular turnover rate if it is both numerous and possesses a relatively short lifespan. The main cell types that our analysis focused 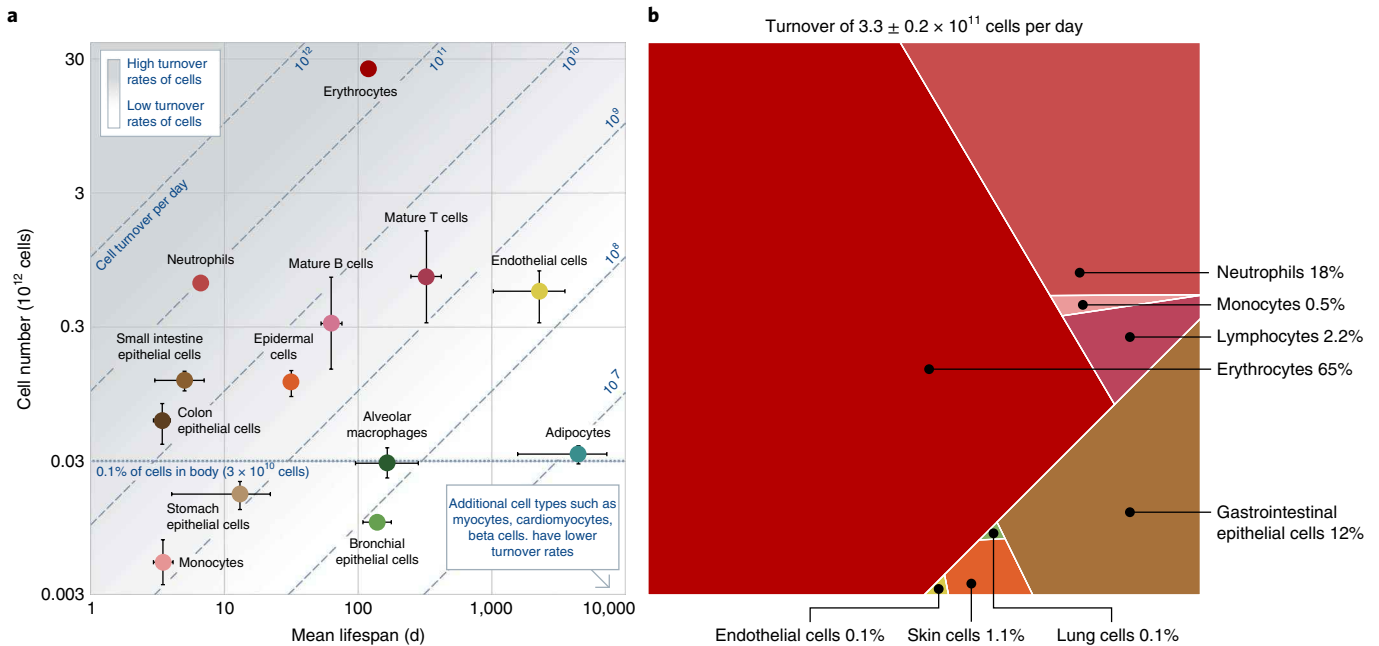on are those comprising at least 0.1% of the 30 trillion cells comprising the human body[3] or ones with an especially fast turnover of $\tau < 10$ d.

We analyzed many of the tissues thought to be relevant and found them to make a negligible contribution in terms of both number and mass (Supplementary Tables 1–4); for example, sperm cells, kidney cells and osteocytes. For cell types with a short lifespan, we revised earlier estimates[1,3] of the total cell number, as documented in Methods. Figure 1a presents for each of these cell types, the number of cells and their mean lifespan (Methods). The ratio between these two parameters gives the overall daily cellular turnover rate. By summing the daily cellular turnover rates for each cell type, we were able to map their contribution to the overall daily turnover rates of human cells (Fig. 1b). To simplify the presentation, we grouped some cell types together (for example, intestinal and stomach epithelial cells, lung cells and lymphocytes). The cellular turnover time is defined based on cell death and not on cell differentiation. For example, in our analysis of blood cells, we included their time as undifferentiated progenitors in their overall cell lifespan (Methods).

We found that the total turnover rate of the human body is $0.33 \pm 0.02 \times 10^{12}$ (330 ± 20 billion) cells d^{-1} (equal to about 4 million cells s^{-1}). About 86% of these cells are blood cells, mostly of bone marrow origin. Almost all of the remaining 14% are gut cells. The three major contributors to the cellular turnover of the human body are jointly responsible for about 96% of the total turnover: erythrocytes (RBCs), neutrophils and intestinal and stomach epithelia.

We define the cellular mass turnover rate as the mean total mass of cells from a specific cell population (most commonly a certain cell type) that die (or are shed) per unit of time. Assuming a characteristic cellular mass, m, for a cell type comprising n cells with a mean lifespan of τ days, the cellular mass turnover rate for the cell type is $\mu = mn/\tau = \beta m$. Note that this definition addresses only the replacement of whole cells, not the intracellular turnover (such as protein turnover in muscle or liver cells) and it does not include the change in mass involved in the growth of existing cells (for example, the enlargement of adipocytes). In line with our definition, we are only concerned with the balance between the mass of cells that die and those replacing them. By combining the cellular turnover rates thus calculated with the mean mass of different cell types[3,5–9], we were able to calculate the contribution of various tissue types to the whole human cellular mass turnover, presented in Fig. 2.

The total turnover rate of human cellular mass is 80 ± 20 g d^{-1}. Despite their ubiquity, blood cells account for only ≈40% of the total cellular mass turnover, due to their relatively low cellular masses of ≈100–300 pg. This contrasts with their ≈80% dominance over total cellular turnover. The epithelial cells of the gastrointestinal tract also contribute about 40% of the cellular mass turnover because of their greater single cell unit mass (≈1,000 pg) and short lifespan. Note that due to their exceptionally long lifespans, adipocytes and

Department of Plant and Environmental Sciences, Weizmann institute of Science, Rehovot, Israel. ✉e-mail: ron.milo@weizmann.ac.il

Fig. 1 | The turnover rates of cells in the human body. a, Number of cells versus mean lifespan for the main human cell types. The center of the points represents the estimate of the mean. For the number of values (*n*) used in deriving the average per cell type see Methods and Jupyter notebooks. Error bars represent the s.e. of the estimates. In some cases the uncertainty is smaller than the marker size. Dashed diagonals indicate an equal daily cellular turnover rate. **b**, The distribution of the daily cellular turnover rate of human cells by cell type. Each polygon area represents the fraction of total daily cell replacement for which the respective cell category accounts. Visualization performed using the online tool at http://bionic-vis.biologie.uni-greifswald.de/. A more highly resolved view, including cell types with relatively small contributions, is provided in Extended Data Fig. 1. About 86% of the cells that are being turned over are blood cells, and in young children an even higher predominance of blood cells in the total cellular turnover is estimated (Methods).

muscle cells contribute only around 5% to the total mass turnover, although they represent ≈75% of the total cellular mass.

For some cell types, we could not locate reliable turnover rates in humans in the literature. We were still able to derive an upper bound based on lifespan estimates from rodents, described in detail in Supplementary Table 2, as the lifespan in humans, in general, exceeds that in rodents. Summing over all potentially relevant cell types, we found an upper bound for the additional total turnover rate of 0.02×10^{12} cells d^{-1}, and in terms of mass, 17 g d^{-1}, with most of the additional turnover due to lung cells and hepatocytes. These values are within the uncertainty range that we report (Methods).

How do the above human cell turnover rates compare with those of the bacteria inhabiting our body? The vast majority of human-associated bacteria, some ≈38 ± 10 trillion cells, reside in the colon and weigh in total ≈200 g (refs. [3,10]). Bacteria doubling times are hard to measure in the natural gut environment. Yet recent metagenomics-based methods enable some overall estimates[11,12], albeit with large uncertainties and yield a timeframe of 2.5–20 h, based on stool samples[13]. Using this range together with the overall bacteria numbers in the gut, we can infer the production of $0.5–4 \times 10^{14}$ bacterial cells, equal to $250–2,000$ g d^{-1}. However, because this approach relies on measurements taken from stool samples, the calculated mass may be an overestimate, as it may not adequately represent the total population of the colon, where some layers of bacteria could adhere to epithelial cells and possibly divide much slower. An adult human produces, on average, 100–200 g of wet stool per day[14], half of which is bacteria[10]. Hence, we can infer an extreme lower bound of total daily turnover of at least 60 g (1×10^{13} cells), reflecting the bacteria in the stool and assuming no bacterial cell turnover in the gut. We thus find that the mass of bacteria produced in the body per day is at least in the order of magnitude of the produced mass of all human cells combined during the same period of time and may be an order of magnitude larger.

Overall, we find that a reference 70 kg person with 30 trillion host cells and 46 kg of cellular mass (the other 24 kg are due to extracellular fluids and solids) produces this number of cells every 80 d and this amount of cellular mass every year and a half. The difference in timescales arises because most of the turnover occurs in small-to-medium cells, whereas much of the cellular mass is concentrated in relatively heavy cells with mean lifespans exceeding 10 years. However, not all parts of the human body are ever replaced (for example, most brain neurons and cells of the eye lens, which we calculate to constitute altogether ≈0.5% of the cells in the human body[15,16]) and hence complete turnover never happens.

In this research, we provide a comprehensive quantitative description of cell turnover in the human body and its distribution across cell types for a healthy 'characteristic' adult. In addition to age and sex factors described in Methods, medical conditions could also affect the turnover. For example, neutrophil lifespan is extended in cases of injury and inflammation[17,18], anemia leads to shortening of the lifespan of erythrocytes[19] and psoriasis leads to a substantial reduction in epidermal cell lifespan[20]. Furthermore, cell turnover is directly linked to cancer[21] and the cell turnover within a tumor may be much faster[22].

Regarding the overall turnover of cellular mass, we find that the rate of homeostatic cellular mass turnover in adults is much higher than the rate of mass accumulation for infants and children aged 9 months through 18 years, as percentage of body mass (Methods). However, it should be noted that the production of new cells is only one of several mass fluxes in the body. For example, fat cell numbers remain relatively constant after maturity, but can undergo alterations in cell size. Much of the normal homeostatic metabolic flux occurs in nondividing cells and is thus not included in this study. In fact, our estimate suggests that the amount of power needed to generate the cells that are being turned over is only a small fraction of the body's power consumption at rest (Methods). We also note that
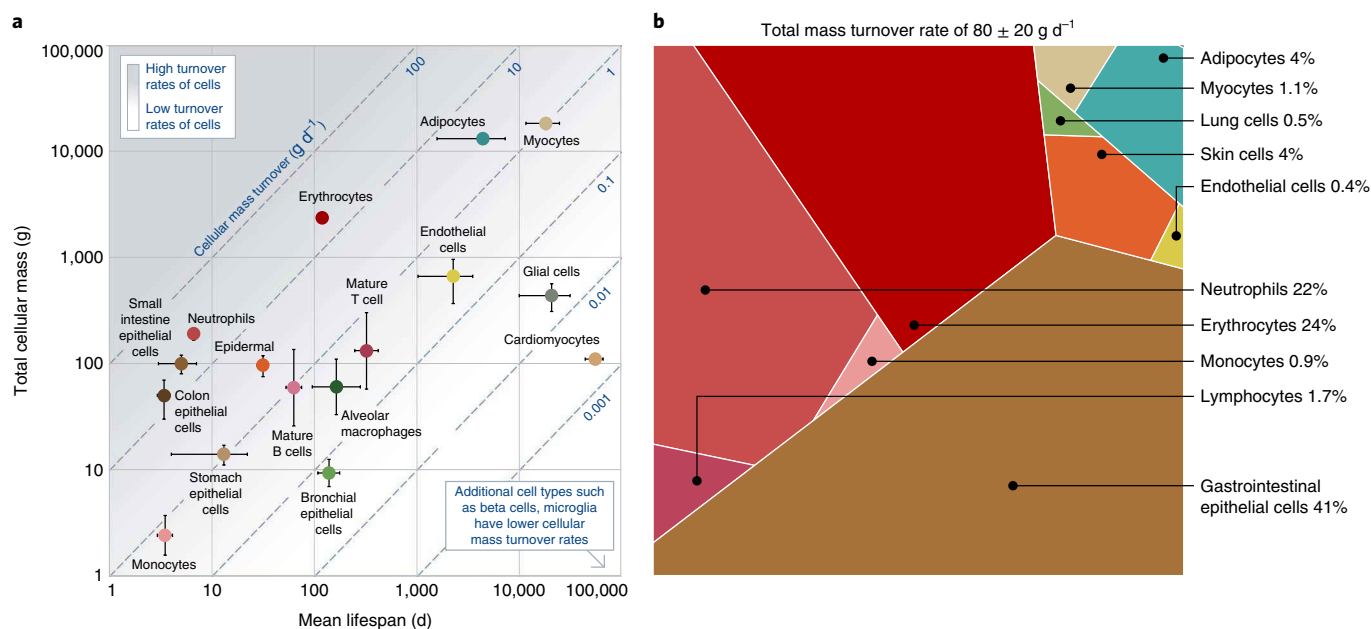
Fig. 2 | The turnover rates of cellular mass in the human body. a, Cellular mass versus mean lifespan for the main human cell types. Cellular mass was taken as the number of cells multiplied by the average mass of cells. The center of the points represents the estimate of the mean. For the number of values (*n*) used in deriving the average per cell type see Methods and Jupyter notebooks. Error bars represent s.e. of estimates. In some cases the uncertainty is smaller than the marker size. Dashed diagonals indicate equal daily cellular mass turnover, with the ratio of the numerical values on the vertical and horizontal axes. **b**, Voronoi tree map of daily mass turnover of human cells by cell type, where each polygon area is proportional to the total mass of the respective cells being replaced daily. A more highly resolved view, including cell types with relatively small contributions, is provided in Extended Data Fig. 2. In women a similar yet slightly smaller role is played by blood cells in the overall cell mass turnover, but without a notable change in the total cellular mass turnover compared to a men of the same weight (reduction of <5%).

the distinction between cellular turnover and metabolic flux within existing cells can sometimes be subtle, such as in the case of estimating turnover time of muscle cells based on radioisotope labels, which tends to indicate nuclei turnover rather than whole-cell turnover.

There are many questions surrounding the topic of organism renewal in health and disease that can be informed by our analysis. For example, how does the turnover of tumor cells compare to the total cellular turnover of the patient's body? What is the energetic and biosynthetic toll of tumor growth and does it directly impact resource allocation, perhaps by commandeering resources otherwise dedicated to tissue regeneration? Quantification of cellular death within different tissues, in combination with emerging cell atlases, can rationalize benchmark values for monitoring tissue-specific biomarkers in the blood, such as circulating DNA and microR-NAs[23]. Deviations from these could signify specific tissue damage as demonstrated, for example, for cancerous conditions[24].

Our analysis also offers an additional aspect to the classic analogy in the metaphysics of identity[25] of the human body as being akin to the ship of Theseus, where all the components are replaced while the identity is paradoxically retained. As shown here, we can now quantitatively dissect what fraction is replaced and on what timescale. Most broadly, the analysis presented here grounds our understanding of and contextualizes questions about the cellular dynamics of the human body in rigorous quantitative terms.

Online content

Any methods, additional references, Nature Research reporting summaries, source data, extended data, supplementary information, acknowledgements, peer review information; details of author contributions and competing interests; and statements of data and code availability are available at https://doi.org/10.1038/s41591-020-01182-9.

References

1. Bianconi, E. et al. An estimation of the number of cells in the human body. *Ann. Hum. Biol.* **40**, 463–471 (2013).
2. Sender, R., Fuchs, S. & Milo, R. Are we really vastly outnumbered? Revisiting the ratio of bacterial to host cells in humans. *Cell* **164**, 337–340 (2016).
3. Sender, R., Fuchs, S. & Milo, R. Revised estimates for the number of human and bacteria cells in the body. *PLoS Biol.* **14**, e1002533 (2016).
4. Snyder, W. S. et al. *Report of the Task Group on Reference Man. Annals of the ICRP/ICRP Publication* vol. 23 (Pergamon Press, 1975).
5. Crosby, W. H. et al. A concept of the pathogenesis of anemia applied to disorders of the intestinal mucosa. *Am. J. Dig. Dis.* **6**, 492–498 (1961).
6. Kuse, R., Schuster, S., Schubbe, H., Dix, S. & Hausmann, K. Blood lymphocyte volumes and diameters in patients with chronic lymphocytic leukemia and normal controls. *Blut* **50**, 243–248 (1985).
7. Ting-Beall, H. P., Needham, D. & Hochmuth, R. M. Volume and osmotic properties of human neutrophils. *Blood* **81**, 2774–2780 (1993).
8. Crapo, J. D., Barry, B. E., Gehr, P., Bachofen, M. & Weibel, E. R. Cell number and cell characteristics of the normal human lung. *Am. Rev. Respir. Dis.* **125**, 740–745 (1982).
9. Stone, K. C., Mercer, R. R., Gehr, P., Stockstill, B. & Crapo, J. D. Allometric relationships of cell numbers and size in the mammalian lung. *Am. J. Respir. Cell Mol. Biol.* **6**, 235–243 (1992).
10. Stephen, A. & Cummings, J. The microbial contribution to human faecal mass. *J. Med. Microbiol.* **13**, 45–56 (1980).
11. Korem, T. et al. Growth dynamics of gut microbiota in health and disease inferred from single metagenomic samples. *Sci.* **349**, 1101–1106 (2015).
12. Brown, C. T., Olm, M. R., Thomas, B. C. & Banfield, J. F. Measurement of bacterial replication rates in microbial communities. *Nat. Biotechnol.* **34**, 1256–1263 (2016).
13. Gibson, B., Wilson, D. J., Feil, E. & Eyre-Walker, A. The distribution of bacterial doubling times in the wild. *Proc. R. Soc. B Biol. Sci.* https://doi.org/10.1098/rspb.2018.0789 (2018).
14. Cummings, J. H., Bingham, S. A., Eastwood, M. A. & Heaton, K. W. Fecal weight, colon cancer risk, and dietary intake of nonstarch polysaccharides (dietary fiber). *Gastroenterology* **103**, 1783–1789 (1992).

15. Lynnerup, N., Kjeldsen, H., Heegaard, S., Jacobsen, C. & Heinemeier, J. Radiocarbon dating of the human eye lens crystallines reveal proteins without carbon turnover throughout life. *PLoS ONE* **3**, 1–3 (2008).
16. Spalding, K. L., Bhardwaj, R. D., Buchholz, B. A., Druid, H. & Frisén, J. Retrospective birth dating of cells in humans. *Cell* **122**, 133–143 (2005).
17. Colotta, F., Re, F., Polentarutti, N., Sozzani, S. & Mantovani, A. Modulation of granulocyte survival and programmed cell death by cytokines and bacterial products. *Blood* **80**, 2012–2020 (1992).
18. Kim, M. H. et al. Neutrophil survival and c-kit+-progenitor proliferation in *Staphylococcus aureus*-infected skin wounds promote resolution. *Blood* **117**, 3343–3352 (2011).
19. Dinant, H. J. & de Maat, C. E. M. Erythropoiesis and mean red-cell lifespan in normal subjects and in patients with the anaemia of active rheumatoid arthritis. *Br. J. Haematol.* **39**, 437–444 (1978).
20. Weinstein, G. D., McCullough, J. L. & Ross, P. A. Cell kinetic basis for pathophysiology of psoriasis. *J. Invest. Dermatol.* **85**, 579–583 (1985).
21. Tomasetti, C. & Vogelstein, B. Variation in cancer risk among tissues can be explained by the number of stem cell divisions. *Science* **347**, 78–81 (2015).
22. Rew, D. A. & Wilson, G. D. Cell production rates in human tissues and tumours and their significance. Part II: clinical data. *Eur. J. Surg. Oncol.* **26**, 405–417 (2000).
23. Landgraf, P. et al. A mammalian microRNA expression atlas based on small RNA library sequencing. *Cell* **129**, 1401–1414 (2007).
24. Thierry, A. R., El Messaoudi, S., Gahan, P. B., Anker, P. & Stroun, M. Origins, structures, and functions of circulating DNA in oncology. *Cancer Metastasis Rev.* **35**, 347–376 (2016).
25. Nozick, R. *Philosophical Explanations* (The Belknap Press, 1981).

Methods

Methods used in the literature for measuring the lifespan and turnover of cells. Cellular turnover was studied in the 1950s[26] and earlier. The main methods utilized both then and now to determine the lifespan of a certain cell type include three stages: (1) Incorporating a radioisotope label, such as ^{51}Cr, ^{3}HTdR (methyl-tritiated thymidine) into the cells of interest; (2) Tracking the label concentration over days, months or even years; and (3) Fitting the data to a model of cellular lifespan, yielding a survival function that determines the probability of a cell to attain a given age[27].

Over the years, concerns have been raised regarding the impact of label toxicity on cell lifespan (for example, ^{3}HTdR for neutrophils[28]). In response, new methods use nontoxic labels, such as deuterium[29] in ^{2}H$_2$O. A particularly celebrated label used for determining turnover of large tissues was environmental ^{14}C, produced by above-ground nuclear weapon testing between the mid-1950s and early 1960s, before this was banned by international treaties. For example, incorporating ^{14}C from the atmosphere into DNA enabled Spalding[16] to determine the mean age of cells in the brain, adipose tissue and skeletal muscle. While in some cases the mathematical model of the survival of cells with time is relatively simple, in other cases it can be complex and include multiple steps and parameters. The uncertainties associated with each model vary widely and, while in our calculations we took preliminary note of this variability, their full effects require further work.

In previous studies, the overall cellular turnover rate was estimated only for a limited fraction of tissues, mainly blood cells and specifically erythrocytes (with a turnover of 200–250 billion cells per day[30]). Additional claims regarding the overall cellular turnover in the body are presented occasionally (for example, 'as many as 10^{11} cells die in each adult each day and are replaced by other cells'[31], 'millions of cells die every minute'[32], '1 million cells per second'[33]), but without any documented source. Hence, a census that offers a holistic view of the turnover rates of different types of cells in the human body is lacking.

Cell types chosen for main analysis. Following Sender et al., 2016 (ref. [3]), we characterized the daily human cell turnover for all cell types that contribute ≥0.1% to the total cell population by applying the equation $\beta = n/\tau$, where β is the cellular turnover rate, n is the number of cells and τ is the mean lifespan of each cell type, estimated based on a survey of the literature. Lifespan of a cell was defined as the length of time since its last division until its death (regardless of intermediate steps of cell differentiation). For stem cells (whose quantities are relatively small), we assumed a lifespan equal to the age of the reference person. As cell types with very short lifespans can substantially affect the overall turnover, even if they comprise <0.1% of the total cell population, which was our original cutoff for analysis, we added all cell types with $\tau < 10$ d (for example, gut epithelia) to our survey to improve the overall accuracy of the analysis, revising their earlier[1,3] total cell count estimates, as shown below.

Cell lifespan data were collected through a literature survey, centered only on direct measurements in humans. Google Scholar was used to search for sources regarding the dynamics of different tissues or cell types using the name of a certain organ/tissue/cell type in combination with one of the following terms: 'lifespan'/'life span', 'turnover', 'proliferation', 'production', 'cell death', 'kinetics' and 'dynamics'. Names of certain relevant methods for the measurements of cell dynamics (for example, '14C', 'BrdU labeling', 'modeling', 'Ki67') were also included in cases where irrelevant results were obtained. The lifespan was estimated from the measurement (given in the original terms of turnover rate, proliferation rate, death rate, labeling index or lifespan) based on the relevant simple model of the tissue (which may contain separate compartments for defined populations), presented in detail below and in Jupyter notebooks. In some cases (alveolar epithelial cells, hepatocytes and dermal fibroblasts), the only available data were measurements in rodents. In these instances, the cell lifespan in rodents was not used in our turnover estimates, only in the uncertainty estimates. An upper bound for the total turnover of a cell type can be derived using rodent data, as a cell's lifespan in rodents is generally shorter than in humans.

An example of the higher resolution achieved by including short-lived cells is our turnover analysis of white blood cells, such as neutrophils and lymphocytes whose differentiation into mature cells includes several phases, during which many cells die rapidly by a selection process. For such cell types, we integrated data on the different stages into a precise estimate of their mean lifespan and separately counted the cells that die at each stage (presented in detail below). For a simpler presentation, we grouped cell types by tissue type or by broader categories (for example, lung cells and lymphocytes, respectively). In tissues with a single dominant cell type in terms of quantity (>80%), the name of the specific cell type is used. A more highly resolved view, including cell types with relatively small contributions, is provided in Extended Data Figs. 1 and 2. In total, our integrated dataset contains data regarding ≈70 cell types, based on ≈80 different sources, provided in full in Supplementary Tables 1–4.

All data extraction and statistical analyses were conducted in Microsoft Excel (Microsoft Excel 2016 MSO 32 bit, Microsoft Corporation. Available at https://office.microsoft.com/excel) and Python programming language v.3.7.9 (Python Software Foundation, https://www.python.org).

Calculation of intracellular mass of tissues using potassium content. To distinguish between the intra- and extracellular portions of each tissue, we leveraged total body potassium measurements. The concentration of potassium in the intracellular and extracellular volumes of the body is known to be relatively constant. Given these constant values, Wang et al.[34] derived a formula connecting the potassium level of a tissue with its nonfat cell mass. The extracellular potassium concentration is only about 3% of the intracellular concentration and thus can be neglected to give the relation: M_{tissue} (kg) = 0.0092 (kg mmol^{-1}) × [K] (mmol).

For most cell types, we derived the overall cellular mass from reports regarding the average cell mass. We then used the potassium content[4] to derive the intracellular mass through the relation described above, as a sanity check. For the cell types for which we could not find relevant cell mass values in the literature (brain cells and myocytes), we relied entirely on Wang and colleagues' method[34] to estimate their cellular mass.

Detailed calculations of cellular turnover for the major contributing tissues. *Erythrocytes.* The most abundant cell type in the body[3], RBCs are the principal means of delivering oxygen to the body's tissues, achieved via transport through the circulatory system. They are formed from stem cells inside the bone marrow, via multiple differentiation steps.

We first computed the turnover rate from the population of circulating cells in the blood and then compared it to a sanity check based on bone marrow RBC progenitor data.

Blood erythrocyte calculations. We calculated the number of circulating erythrocytes by multiplying their concentration by the blood volume. We calculated the mean blood volume using several formulas connecting it to whole-body properties, such as mass and height[4,35]. The mean concentration of RBCs was likewise taken as the average of reference values for the body's blood count from literature (see detailed references in Jupyter notebooks).

Over the years, the lifespan of circulating RBCs was estimated by numerous experiments, most of them based on labeling methods (pulse chase). It seems that many of the older labeling methods made use of radioactive substances that may have affected, due to their poisonous effects, the cell lifespan and consequently, the obtained values. Recent research has used nontoxic substances, such as ^{2}H$_2$O. We used a recent analysis[27] that modeled the lifespan of blood RBCs using different assumptions regarding its distribution, based on data from previous labeling experiments using ^{2}H$_2$O. We used the estimates from their three models (all of which fit well with the data) and averaged them to receive a mean lifespan of 116 ± 3 d for blood erythrocytes.

Using the estimate for total number and mean lifespan of blood erythrocytes, we calculated a cellular turnover of $2.1 \pm 0.1 \times 10^{11}$ cells d^{-1}. Combined with an average mass of 94 ± 4 pg, we calculated a cellular mass turnover rate of 20 ± 1 g d^{-1} for blood RBCs.

Bone marrow RBC progenitors: sanity check for the turnover of blood RBCs. In steady state, the number of RBCs produced in the bone marrow is equal to the number of RBCs that die. There are limited data regarding the size of the RBC progenitor population in the bone marrow, so we used existing data as a sanity check for the previous calculation. We used data from two sources regarding the number and distribution of RBC progenitors in bone marrow (total of $3.1 \pm 0.5 \times 10^{11}$) and their generation time (see detailed references in Jupyter notebooks).

Neutrophils. The most abundant type of granulocyte, neutrophils are an essential part of the innate immune system. Formed from hematopoietic stem cells inside the bone marrow, they are short-lived and highly motile, as they can enter parts of the tissue where other cells cannot.

The estimate of neutrophils' daily turnover was made in two parts:

1. We surveyed the literature for data regarding the number of neutrophils, separately for each differentiation stage from hematopoietic stem cells. We concluded the total number of cells in each stage.
2. We gathered data regarding the lifespan of neutrophils from papers published in the last 50 years. As the old measurement methods seemed to have biases, we based our values on recent models.

Neutrophil number and distribution calculations. Most of the neutrophils reside in the bone marrow. They can be separated into four major groups, which correspond to different life stages:

1. Mitotic pool: stem cells and progenitor cells that undergo mitosis and so create new cells that in turn, differentiate.
2. Post-mitotic pool: cells that still reside in the marrow but do not undergo mitosis anymore, just differentiate for several days, until they get to the mature neutrophil stage.
3. Circulating pool: mature neutrophils that circulate in the blood.
4. Marginal pool: mature neutrophils that move from the blood into different tissues in the body, where they reside until they die.

Data regarding the overall number of neutrophils and their distribution were taken from five sources that spanned a 50-year period (see detailed references in

Jupyter notebooks). Original values are given as cells kg^{-1} of body weight. We used 70 kg to obtain reference values for humans.

Neutrophil lifespan and turnover calculations. Neutrophils are known to be short-lived and for the past decades were believed to have a half-life <7 h. However, recent studies have shown different results, some diverging by orders of magnitude.

According to Tak et al.[28], the old measurements that relied on an ex vivo/in vivo labeling method with radioactive tracers, like $DF^{32}P$ or ^3HTdr, had an effect on the results and were biased for low values. In recent years, some new methods were developed, using in vivo deuterium labeling with ^2H. This relatively new technique labels cells without cytotoxic effects. Recent papers[36,37] used measurements taken with these new methods combined with detailed models of different pools to arrive at more precise estimates.

It should be noted that the assumptions underlying the detailed models used to interpret the results are especially important. According to Turner et al. and Lahoz-Beneytez et al.[36,38], there is a mistake in Pillay et al., 2010 [37], which involves the assumption that there are much more cells in the blood than in the mitotic pool. This mistake caused a large overestimate of lifespan.

We used the values from Lahoz-Beneytez et al.[36], as they were measured using the new method and the paper provided the largest number of details. We used as a reference the average values of three models that they employed. Mean lifespan in the blood is derived from half-life data using the proportion between the mean lifespan in their model and in a simple exponent model, calculated for a given value for one of the models. From three values of 13-, 16- and 19-h half-life in the blood, we get a mean lifespan of 0.9 ± 0.1 d in the blood.

In addition, Lahoz-Beneytez et al.[36] gives a value of 5.7 ± 0.1 d for post-mitotic transit time.

We obtained a total neutrophil cell turnover rate of $6 \pm 1 \times 10^{10}$ cells d^{-1} from the average of two estimates: bone marrow pool and circulating pool (including blood and marginal pools).

Using a cell mass of 300 pg[7], we translated neutrophil turnover to terms of mass: 18 ± 4 g d^{-1}.

Gastrointestinal epithelial cells. Previous estimates of the number of intestinal epithelial cells in the human body have ranged from 2×10^{10} to 7×10^{11} (refs. [1,5]), most of which are in the small intestine, with a negligible contribution from stomach cells. We have updated the estimates of the number of cells in the different segments of the gastrointestinal tract and have combined them with lifespan data to generate a revised estimate of the cellular turnover rate of gastrointestinal epithelial cells.

Small intestine calculations. The small intestine is responsible for most of the surface area of the gastrointestinal tract. We used several methods to determine the number of cells it houses:

- Estimation using villus and crypt numbers and their enterocyte content. Villus and crypt geometric parameters such as height (depth for crypt) and width were taken from the literature. When there were no concrete data from human research, data were taken from animals (see detailed references in Jupyter notebooks). In the first method, the volumes of the villi and crypts were calculated from geometric features and the number of enterocytes in each were estimated by division by the respective calculated cell volume[5]. In the second method, the enterocyte content of each villus and crypt was derived from the surface area, calculated from geometric features and divided by the surface area of a single enterocyte. In both methods, the enterocyte content of a single villus was multiplied by the total number of villi[5] and the enterocyte content of a single crypt was multiplied by the number of crypts, derived from the crypt-to-villus ratio[39]. Using these two methods, we determined the number of enterocytes in the small intestine to range between 0.9–1.2×10^{11}.
- Estimation using slices from the mucosa, based on previous work[40,41]. In these studies, muscularis mucosae slices of 10^4 μm^2 were taken and separated in a different mucosa component. The volume of the epithelium was measured and divided by the volume of a single epithelial cell to arrive at the area density in the small intestine. Multiplying this figure by the total surface area of the small intestine (not including the factors of the villi and microvilli) yielded an estimate of 1.3×10^{11} enterocytes in the small intestine.

By taking the average of the three calculated values, we arrived at a revised estimate of $1.2 \pm 0.2 \times 10^{11}$ small intestine epithelial cells.

The mass of the small intestine epithelial cells was estimated based on their size[40] and was used also for the similar epithelial cells in the colon.

Stomach calculations. To estimate the number of relevant epithelial cell (with fast turnover) in the stomach, we used data regarding the mass composition of the stomach and the various cell types' contribution[42]. There are several types of cells in the stomach epithelium, most of which have a turnover of ~40–70 d (measured in mice)[43], so here we describe only our estimates of the mucous surface cells (henceforth 'stomach epithelial cells' unless mentioned otherwise), which are similar to the small intestine enterocytes and have a turnover of ~10 d.

To estimate the cellular mass of the stomach epithelial cells, we used the average total mass of the stomach[44] combined with data regarding the percentage of mass contained in the stomach mucosa, especially in the relevant cells[42]. However, the data we used[42] were taken from the corpus, which comprises only 80% of the stomach. We extrapolated the cellular mass of the other 20% using different assumptions regarding its cellular composition, based on the fact that in these other segments (cardia and pyloric) there are no enzyme-secreting cells, only epithelial cells (mucous surface and neck cells). We obtained two boundaries using different assumptions regarding the ratio of these types of cells and averaged them to get a reference estimate for the total cellular mass of mucous surface cells, with its uncertainty. We then used data regarding the size of mucous surface cells to conclude an estimate for the total number of mucous surface cells in the stomach: $1.7 \pm 0.4 \times 10^{10}$.

Colon calculations. To estimate the number of cells in the colon, we used data regarding the area density of crypts together with estimates of the surface area of the colon and the number of cells in a given crypt (see detailed references in Jupyter notebooks). We reached a total of $5.6 \pm 2 \times 10^{10}$ colon epithelial cells. We then use estimates based on extrapolation from rats[45] as a sanity check.

Lifespan and turnover calculations for gastrointestinal epithelial cells. To calculate the lifespan of the gastrointestinal epithelial cells, we reviewed several sources gathered in a recent meta-analysis[46] (see detailed references in Jupyter notebooks). As the integrated data in Darwich and colleagues'[46] supplementary information contains several measurements that are not the lifespan or turnover of the epithelial cells (such as generation or cell cycle times), we chose only relevant measurements concerning the epithelial cells in the stomach, small intestine and colon. From each data source, we extracted the mean value, number of patients (n) and method of measurement (only some included the s.d. of results). Except for the small intestine, each segment of the gastrointestinal tract has data derived by two different measurement methods.

We estimated the mean turnover of epithelial cells for each gastrointestinal tract segment in two stages. First, we aggregated the results according to the measurement methods. For each method used, we derived the mean turnover measured and its s.e.m. by weighted average, considering the number of patients and the reported s.d. Second, we averaged the values between the different methods (simple arithmetic mean) and propagated the errors, considering two sources of uncertainty:

a. Intra-method error: errors between different measurements using the same method.
b. Inter-method error: difference between values of two methods.

Extended Data Fig. 3 presents the distribution of values taken from the literature sources and the mean calculated in the described technique.

Using this derivation, we estimated the lifespan of the cells to be 13 ± 9 d in the stomach, 5.3 ± 1.7 d in the small intestine and 3.4 ± 0.5 d in the colon.

Based on the above estimates of the number of cells and their lifespan, a total cellular turnover rate of $1.3 \pm 0.9 \times 10^9$ cells d^{-1} in the stomach, $2 \pm 1 \times 10^{10}$ cells d^{-1} in the small intestine and $1.7 \pm 0.6 \times 10^{10}$ cells d^{-1} in the colon was obtained. The cellular mass turnover rates are 1.1 ± 0.7, 19 ± 8 and 14 ± 6 g d^{-1}, for the stomach, small intestine and colon, respectively.

Lymphocytes. Lymphocytes comprise about 3.5% of the cells in the body. Lymphocyte differentiation and maturation is a complex process, with some cells rapidly being replaced. To discern these processes, we reviewed separately the differentiation and maturation process of B and T cells and accounted for their death rate in the various stages of each process. From the death rate, we calculated turnover rate and mean lifespan. Most of the literature regarding the processes and rates is from the 1980s and 1990s and is based on studies conducted on mice and rats. Hence, we could only obtain complete (based on measurements in humans) estimates of mature B and T cells. In addition, we were able only to extrapolate the turnover of lymphocyte progenitors, based on data from rodents.

Lymphocyte number and distribution calculations. Over the years, there were several attempts to estimate the number and distribution of lymphocytes in the human body. The dominant sources regarding the number and spatial distribution of lymphocytes in humans is Trepel[47], who based his estimates mainly on extrapolation from cell density measured in rats (at a total of about 0.5×10^{12} cells). However, later research on monkeys[48] demonstrated that larger lymphocyte densities could be found in the spleen and other organs, leading to an updated estimate of 1.9–2.9×10^{12} cells. As both studies use rely on nonhuman organisms to derive their estimates, we chose to refer to the average of these estimates and include a large range for errors.

The distribution of T cells, B cells and natural killer cells is taken from research conducted on humans[49]. Data regarding the lymphocyte population distribution in different tissues were integrated with data regarding their overall numbers according to a method used in the literature[50], resulting in overall estimates of 7×10^{11} T cells, 3×10^{11} B cells and 0.5×10^{11} natural killer cells, with a multiplication uncertainty factor of 2.2 (for $1 \times$ s.d.).

Mature lymphocytes lifespan and turnover calculations. The B and T cells in the mature pool are divided into categories according to their function, mainly naive

and memory cells. We used data from several studies that measured the death and proliferation of B and T cells using labeling with ^{2}H in glucose or water. These experiments usually measured the level of labels over a period of several weeks. We based our analysis on the sources selected in the review by Borghans et al.[51]. Their inclusion criteria were related to the labeling technique and length of the experiment.

We used reference data taken from blood for the relative fraction of the different T and B cell subpopulations. Note that the two sources used different schemes to differentiate between subpopulations and so we only concentrated on the three subpopulations for which we had proliferation-rate data. Integrating the lifespans with the number of cells, representing the cellular mass derived from five sources (see detailed references in Jupyter notebooks), we obtained the following total turnover rates: 5×10^9 B cells or 0.9 g B cells d^{-1}, 2×10^9 T cells or 0.4 g T cells d^{-1}.

Lymphocyte progenitor lifespan and turnover calculations. Here we present the maturation progress of lymphocytes and extrapolate the death rate of progenitors based on studies in rodents.

B cells differentiate in the bone marrow in a process involving several stages. Pro-B are mitotic stages (two stages in rats, three in mice) that produce new cells, which go through further selection to Pre-B cells (large Pre-B cells are mitotic and they mature into small Pre-B cells, which are nonmitotic, still in the bone marrow). Pre-B cells go through an additional selection process, with those successful reaching the stage of immature B cells. Considering the data regarding the production rates of Pro-B and large Pre-B cells in mice and rats (see detailed references in Jupyter notebooks), we can see that the flux of nonmitotic cells is lower than the potential of cells being produced daily by mitosis, indicating that most of the cells die rapidly, with a short mean lifespan of ≈ 0.8 d (in mice). From the proportion of lymphoid progenitors out of the total bone marrow nucleated cells we got an estimate of 6×10^9 progenitor B cells. Assuming a lifespan as in rodents, we get an extrapolated cellular turnover rate of 7×10^9 cells d^{-1}. Once the Pre-B cells differentiate into immature B cells they migrate to the spleen and are, thereafter, called transitional B cells. While it was previously supposed that most transitional B cells are removed in the selection process in the spleen, it seems that 60–80% of them do succeed and join the mature B cell pool after a period of about 4 d.

T cells go through a different selection process, which happens mostly in the thymus. The selection process in the thymus is very demanding, with only a few percent (measured in mice) of the thymocytes that enter the thymus completing the process and joining the mature T cell pool. Quantification of the total number of cells in the thymus was performed using data regarding thymic output in humans, with comparison to older references undertaken for the number of lymphocytes in the thymus. Combining the overall number of thymocytes, 2×10^9 cells, with a mean lifespan in mice of ≈ 4 d, we get a potential turnover of 5×10^8 T cells per day.

Epidermal cells. The epidermis, the outer layer of the skin, contains tens of layers of cells, separated into 4–5 domains. The epidermis is populated mostly by nucleated keratinocytes. The top 15–20 layers of cells are called stratum corneum and contain corneocytes, dead keratinocyte cells, which we chose not to include in our estimate, as they are already dead.

In addition to keratinocytes, the epidermis includes several other types of cells, but those have considerably low numbers and a longer lifespan and thus are negligible for the purpose of our analysis.

Epidermal cell number and mass calculations. We combined the data regarding the surface area of the body (1.9 m^2 (ref. [44])) with measurements of cellular area density[52] to get an estimate of the number of different cells in the epidermis. We also used data regarding the prevalence of melanocytes[53] to estimate their minor contributions. Averaging the density from the two sources led to a total of 6.2×10^4 cells per mm^2, 95% of it due to keratinocytes. Multiplying this figure by the surface area of the reference person yields a total of $1.2 \pm 0.3 \times 10^{11}$ nucleated keratinocytes.

We integrated the number of cells with their mean mass to get an estimate of 100 ± 20 g for the total epidermal cellular mass. Another method to estimate the total cellular mass of the epidermis utilizes the measurement of its potassium content[4]. Using the method developed by Wang et al.[34] (described above), we reach an epidermal total cellular mass of 110 ± 40 g, including ≈ 30–40 g of corneocytes. Thus, we get similar estimates for the cellular mass of the epidermis by both methods.

Epidermal cell lifespan and cellular turnover calculations. The lifespan of keratinocytes was estimated in the literature by integrating labeling measurement with modeling of the turnover through three major compartments of the epidermis:

1. Germinative cell layer: the basal layer in which cells are produced.
2. Overlying viable epidermis: the layers in which the keratinocytes are still viable.
3. Stratum corneum: the outer layer, which contains only dead cells (corneocytes).

For the lifespan calculations, we focused only on the first two compartments.

During the 1970s and 1980s, several studies used estimates for the duration of the DNA synthesis (S-phase) and labeling indices, and their relation to the cell cycle, to estimate turnover through the three compartments (see detailed references in Jupyter notebooks). We took their values for the turnover and used the average of the main values (range of 25–38 d) as our reference. Combining the number and mass of the epidermal nucleated cells with their lifespan, we got an estimated epidermal cellular turnover rate of $3.7 \pm 0.9 \times 10^9$ cells d^{-1} or in terms of cellular mass, a turnover rate of 3.1 ± 0.8 g d^{-1}.

Uncertainty estimates. Uncertainty estimates were derived for each cell type based on the uncertainty inferred from the literature regarding the measurement of cell lifespan, number and mass. The overall uncertainty was calculated based on the uncertainty propagation of all individual uncertainty components. Uncertainties are given as $1 \times$ s.e. of the values (also for cases with large uncertainties, given as multiplication factors). All estimate derivations are documented and supplied in Jupyter notebooks (https://github.com/milo-lab/cellular_turnover).

Analysis of the uncertainty in our estimate. This study aims to provide a rigorous holistic view of cellular turnover in the human body with credible uncertainty estimates. As shown in the text, the largest uncertainty factor in our estimates lies in the estimate of the bacterial doubling time in the gut. With two values that differ by an order of magnitude[11,12], the corresponding uncertainty is significantly greater than the total turnover of the human body. Another factor contributing to the uncertainty of bacterial turnover is the fraction of bacteria presented in stool, for which the doubling time was measured. Future efforts to calibrate metagenomic measurements and new quantitative approaches are needed to better support and constrain these values.

Examining the uncertainty in human cell turnover rate in terms of cell type, we found a similar contribution from the four dominant cell types: erythrocytes, neutrophils, lymphocytes and intestine epithelium (both small and large intestine). The uncertainty in the estimates of these cells' turnovers is about 5–25% of their cellular turnover rate. Because of the dominant contribution of erythrocytes to the total turnover rate, which harbors a relatively small degree of uncertainty, the overall uncertainty is small $\approx 10\%$ ($33 \pm 2 \times 10^{10}$ cells d^{-1}). For erythrocytes, which contribute over half the total daily cellular turnover by number, a lifespan of 110–120 d is well established[27,54]. However, the uncertainty values for the lifespan of intestine epithelial cells are relativity large, affecting the uncertainty of the total cellular turnover rate, as they rely on few labeling experiments, most of them with small sample size and could be affected by interpatient variability. The uncertainty of the cellular turnover of neutrophils and lymphocytes stems mainly from the unknowns in the estimate of their number.

The uncertainty of the cellular mass turnover rate is mostly dominated by gastrointestinal epithelial cells (whose daily turnover is 34 ± 10 g d^{-1}). This large uncertainty is mainly due to possible errors in the estimate of their lifespan, cellular mass and number. Further research utilizing new labeling techniques and models to examine the lifespan of these cells could reduce the overall uncertainty of our estimate.

One possible bias in our estimates is the omission of relevant cell types with no known lifespan, despite a possible effect on total turnover estimate. As can be seen in Supplementary Table 4, boundaries for the potential additional cellular turnover due to such exclusions are on par with the uncertainty of our estimates and led us to round the cellular mass turnover uncertainty up to 20 g d^{-1}. A future thorough census of cellular mass of different tissues in the human body and their separation into composing cell types could help complete such an analysis.

Analysis of age and sex effects. The effects of age and sex on cellular turnover can be captured by focusing on three dominant cell types: erythrocytes, neutrophils and intestinal epithelium. Children have a relatively high cellular turnover rate due to a shorter erythrocyte lifespan (60–80 d versus 120 d in adults)[55] and probably a shorter lifespan of intestinal epithelia (shown for mice[56]). Combined with children's high blood-volume-to-weight ratio[44], we predict an even higher predominance of blood cells in total cellular turnover. Furthermore, new findings indicate low division rates of stem cells in older individuals[57], which would significantly decrease their overall cellular turnover rates.

Women also have shorter erythrocyte lifespans, which increases their overall cellular turnover[55] (pregnancy lowers the lifespan of erythrocytes even more[58]). However, the blood volume of women and their RBC counts are lower than those of men. As the sex differences in organs such as the intestine are relatively small, we expect a slightly smaller role for blood cells in overall turnover, but without a significant change in total cellular mass turnover compared to a male of the same weight (reduction of <5%).The effects of ethnicity, obesity and health status require dedicated measurement for further characterization.

Comparison of homeostatic cellular turnover in adults with mass accumulation during early development. We can compare rates of cellular mass turnover to rates of mass accumulation during advanced fetal development and childhood.

Over the third trimester, a fetus acquires an average of 10–25 g of cellular mass per day[44], excluding extracellular mass and cell production in the fetal regenerating

tissues. This corresponds to ≈1% of its total mass. This figure is several times greater than adult mass regeneration rates: about 80 g d⁻¹ or about 0.1% of the total mass (≈0.2% of total cellular mass).

Similarly, during the first 3 months after birth, a neonate weighing 3 kg will, on average, double his or her weight. This indicates a daily increase of ≈30 g d⁻¹ or ≈1% d⁻¹; again, a smaller rate in absolute terms than the cellular mass produced in adults but a few times larger in terms of fraction of body weight.

However, these mass accumulation rates are much higher than what is expected for infants and children aged 9 months through 18 years. As can be seen in Extended Data Fig. 4, the maximal rate of mass production, 30–40 g d⁻¹, is reached in the first 3 postnatal months. After 9 months of age, the relative rate of cellular mass accumulation drops below that of an adult man's homeostatic cellular mass turnover (≈0.2% g of cells per g cellular mass per day). For most of the development period, the relative rate of mass accumulation stays relatively constant, smaller by an order of magnitude than an adult man's homeostatic cellular mass turnover rate, including during puberty.

Estimate of the power consumption involved in homeostatic cellular turnover. We can use considerations of energy and power consumption of the human body and its tissues as reference values for doing a 'sanity check' on our estimate of cellular mass turnover rate. The energetic cost of production and death of cells has been the subject of research over the years, mostly in unicellular organisms, such as bacteria and yeast[59]. Cell production and removal in the body are complex processes that involve many mechanisms at various levels, ranging from the molecular level to that of the entire tissue and even the entire body. Previous analysis[59] has suggested that the main factor affecting energy costs of production of new cells lies in the synthesis of new proteins, as they usually represent the largest fraction of the cellular dry weight[60]. Using the estimate presented in this study of a cellular mass turnover rate of 80 g d⁻¹ (wet weight), we can estimate the power needed to generate this rate of cells by concentrating on the protein portion needed to be synthesized. Considering a 70% cellular water content and a 60% dry-mass proportion of proteins, we get a protein turnover rate of ≈15 g d⁻¹ (which refers only to new cells and not to the turnover of proteins in cells that remain intact). The synthesis of new proteins involves several steps, including the transcription of the gene encoding for the protein, transport of the metabolites needed for the synthesis (mainly amino acids) and the translation and elongation of the peptide. The energetic cost of the primary step of peptide chain elongation has been established (equivalent to 4 ATP per 1 amino acid) and is considered to be the main energetic burden. However, the energetic demands of the other steps are nontrivial. Theoretical analysis[61] and empirical experiments[62] suggest that the overall energetic cost of protein synthesis amounts to 4.5–5.3 kJ g⁻¹ protein, equivalent to 6–7 ATPs per amino acid (using a mean amino acid mass of 106 Da and a free energy for ATP production of −80 kJ mol⁻¹). For the synthesis of ≈15 g protein involved in daily cell production, we get a total power consumption of 15 g d⁻¹ × (4.5-5.3 kJ g⁻¹) × 0.24 kcal kJ⁻¹ = 16–19 kcal d⁻¹. Looking at the two tissues in which >95% of the cells are produced, we get a power consumption of 8–9 kCal d⁻¹ in bone marrow and 7–8 kCal d⁻¹ in the gastrointestinal tract. By comparing these values of power consumption to the resting metabolic rate of the tissues[63] and the whole body[44], we find that the production of new cells represents about 3% of the metabolic rate of the gastrointestinal tract and about 1% of the total metabolic rate of the entire body. It should be mentioned that this estimate is consistent with the notion[64] that the whole-body protein turnover of close to 300 g d⁻¹ demands an energetic cost of about 20% of the total metabolic rate of the body. According to our estimate, about 5% of the whole-body protein turnover is involved in the cellular turnover (≈15 g d⁻¹ out of ≈300 g d⁻¹). Thus, we would expect the protein turnover within the cellular turnover to be associated with an energy cost of 5% × 20% ≈ 1% of the resting energy of the body.

This estimate does not include the energetic costs of organized death and removal of cells. About half of cells replaced daily go through apoptosis and phagocytosis by tissue macrophages (the other half are those of the gastrointestinal tract and skin, which are shed). Although these processes demand energy as well, a quantitative analysis of them is still missing and we assume that they do not have a dramatic effect on the overall calculation. A crude estimate can be established by focusing on the energy needed to degrade proteins in dying cells. As cells undergo phagocytosis, their content is degraded in the lysosomes of engulfing cells. The degradation of a protein in the lysosome is associated with a need to transport its amino acids back out to the cytosol, with an energetic cost of about 1 ATP per 3–4 amino acids[59] (in addition to the energy needed to maintain the lysosomes at low pH levels, which is arguably part of the energy consumption of the cellular turnover). Thus, the energetic cost of degrading a protein included in the cellular mass turnover is on the order of 0.5 kCal d⁻¹. Notably, the energetic cost of lysosomal degradation is similar to the energy cost of degrading this amount of protein by the ubiquitin–proteasome system[65]. This is more than an order of magnitude less than the power needed for synthesis. We assume that other energy costs associated with cellular degradation would not change this overall result.

Reporting Summary. Further information on research design is available in the Nature Research Reporting Summary linked to this article.

Data availability

To generate our estimates of cellular turnover, we extracted values from the literature as detailed in the attached spreadsheet files. Our analysis pipeline consists of about 15 different Jupyter notebooks that use the data extracted from the literature as inputs for generating our estimates. The data extracted for the purpose of our analysis, as well as the results of our analysis are summarized in tables available in the GitHub repository located at https://github.com/milo-lab/cellular_turnover.

Code availability

We provide the code for generating all numeric estimates at https://github.com/milo-lab/cellular_turnover.

References

26. Van Putten, L. M. & Croon, F. The life span of red cells in the rat and the mouse as determined by labeling with DFP32 in vivo. *Blood* **13**, 789–794 (1958).
27. Shrestha, R. P. et al. Models for the red blood cell lifespan. *J. Pharmacokinet. Pharmacodyn.* **43**, 259–274 (2016).
28. Tak, T., Tesselaar, K., Pillay, J., Borghans, J. A. M. & Koenderman, L. What's your age again? Determination of human neutrophil half-lives revisited. *J. Leukoc. Biol.* **94**, 595–601 (2013).
29. Macallan, D. C. et al. Measurement of cell proliferation by labeling of DNA with stable isotope-labeled glucose: Studies in vitro, in animals, and in humans. *Proc. Natl Acad. Sci. USA* **95**, 708–713 (1998).
30. Lockshin, R. A. & Zakeri, Z. Cell death in health and disease: angiogenesis review series. *J. Cell. Mol. Med* **11**, 1214–1224 (2007).
31. Gilbert, S. F. *Developmental Biology* (Sinauer Associates, 2009).
32. Raff, M. Cell suicide for beginners. *Nature* **396**, 119–122 (1998).
33. Han, C. Z. & Ravichandran, K. S. Metabolic connections during apoptotic cell engulfment. *Cell* **147**, 1442–1445 (2011).
34. Wang, Z. et al. Body cell mass: model development and validation at the cellular level of body composition. *Am. J. Physiol. Endocrinol. Metab.* **286**, E123–E128 (2004).
35. Boer, P. Estimated lean body mass as an index for normalization of body fluid volumes in humans. *Am. J. Physiol.* **007**, 632–636 (1984).
36. Lahoz-beneytez, J. et al. Neutrophil kinetics: modeling of stable isotope labeling data supports short blood neutrophil half-lives. *Blood* **127**, 3431–3439 (2016).
37. Pillay, J. et al. In vivo labeling with ²H₂O reveals a human neutrophil lifespan of 5.4 days. *Blood* **116**, 625–627 (2010).
38. Turner, S. M., Emson, C. L., Hellerstein, M. K. & Dale, D. C. Deuterium and neutrophil kinetics. *Blood* **117**, 6052–6054 (2011).
39. Loehry, C. A. & Creamer, B. Three-dimensional structure of the human small intestinal mucosa in health and disease. *Gut* **10**, 6–12 (1969).
40. Crowe, P. T. & Marsh, M. N. Morphometric analysis of small intestinal mucosa IV. Determining cell volumes. *Virchows Arch. A Pathol. Anat.* **422**, 459–466 (1993).
41. Marsh, M. N., Crowe, P. T., Moriarty, K. J. & Ensari, A. Morphometric analysis of intestinal mucosa: the measurement of volume compartments and cell volumes in human intestinal mucosa. in. *Methods Mol. Biol.* **41**, 125–143 (2000).
42. Hogben, C. A. M., H., K. T., Woodward, P. A. & Sill, A. J. Quantitative histology of the gastric mucosa: man, dog, cat, guinea pig, and frog. *Gastroenterology* **67**, 1143–1154 (1974).
43. Forte, J. G. in *Comprehensive Human Physiology From Cellular Mechanisms to Integration* (eds Greger, R. & Windhorst, U.) 1239–1258 (Springer-Verlag, 1996).
44. ICRP. *Basic Anatomical and Physiological Data for use in Radiological Protection: Reference Values. ICRP Publication 89. Annals of the ICRP* vol. 32 (Pergamon, 2002).
45. Mehl, L. E. A mathematical computer simulation model for the development of colonic polyps and colon cancer. *J. Surg. Oncol.* **47**, 243–252 (1991).
46. Darwich, A. S., Aslam, U., Ashcroft, D. M. & Rostami-Hodjegan, A. Meta-analysis of the turnover of intestinal epithelia in preclinical animal species and humans. *Drug Metab. Dispos.* **42**, 2016–2022 (2014).
47. Trepel, F. Number and distribution of lymphocytes in man. A critical analysis. *Klin. Wochenschr.* **52**, 511–515 (1974).
48. Di Mascio, M. et al. Primates non-invasive in vivo imaging of CD4 cells in SHIV infected non-human primates Rockville, MD. *Blood* **114**, 328–338 (2009).
49. Westermann, J. & Pabst, R. Distribution of lymphocyte subsets and natural killer cells in the human body. *Clin. Investig.* **70**, 539–544 (1992).
50. Apostoaei, A. J. & Trabalka, J. R. Review, synthesis and application of information on the human lymphatic system to radiation dosimetry for chronic lymphocitic leukemia. 12–39 (SENES Oak Ridge, Inc. Center for Risk Analysis, 2010).
51. Borghans, J. A. M., Tesselaar, K. & de, B. R. Current best estimates for the average lifespans of mouse and human leukocytes: reviewing two decades of deuterium-labeling experiments. *Immunol. Rev.* **285**, 233–248 (2018).

52. Hoath, S. B. & Leahy, D. G. The organization of human epidermis: functional epidermal units and phi proportionality. *J. Invest. Dermatol.* **121**, 1440–1446 (2003).

53. Quevedo, W. C., Fitzpatrick, T. B., Pathak, M. A. & Jimbow, K. Role of light in human skin color variation. *Am. J. Phys. Anthropol.* **43**, 393–408 (1975).

54. Franco, R. S. Measurement of red cell lifespan and aging. *Transfus. Med. Hemotherapy* **39**, 302–307 (2012).

55. An, G., Widness, J. A., Mock, D. M. & Veng-Pedersen, P. A novel physiology-based mathematical model to estimate red blood cell lifespan in different human age groups. *AAPS J.* **18**, 1182–1191 (2016).

56. Fry, R. J., Lesher, S. & Kohn, H. I. Age effect on cell-transit time in mouse jejunal epithelium. *Am. J. Physiol.* **201**, 213–216 (1961).

57. Tomasetti, C., Poling, J., Roberts, N. J., London, N. R. & Pittman, M. E. Cell division rates decrease with age, providing a potential explanation for the age-dependent deceleration in cancer incidence. *Proc. Natl Acad. Sci. USA* **116**, 20482–20488 (2019).

58. Lurie, S. & Mamet, Y. Red blood cell survival and kinetics during pregnancy. *Eur. J. Obstet. Gynecol. Reprod. Biol.* **93**, 185–192 (2000).

59. Lynch, M. & Marinov, G. K. The bioenergetic costs of a gene. *Proc. Natl Acad. Sci. USA* **112**, 15690–15695 (2015).

60. Feijo Delgado, F. et al. Intracellular water exchange for measuring the dry mass, water mass and changes in chemical composition of living cells. *PLoS ONE* **8**, e67590 (2013).

61. Waterlow, J. C. *Protein Turnover* (CABI, 2006).

62. Aoyagi, Y., Tasaki, I., Okumura, J. & Muramatsu, T. Energy cost of whole-body protein synthesis measured in vivo in chicks. *Comp. Biochem. Physiol. Part A Physiol.* **91**, 765–768 (1988).

63. Aiello, L. C. & Wheeler, P. The expensive-tissue hypothesis: the brain and the digestive system in human and primate evolution. *Curr. Anthropol.* **36**, 199–221 (1995).

64. Welle, S. & Nair, K. S. Relationship of resting metabolic rate to body composition and protein turnover. *Am. J. Physiol.* https://doi.org/10.1152/ajpendo.1990.258.6.E990 (1990).

65. Peth, A., Nathan, J. A. & Goldberg, A. L. The ATP costs and time required to degrade ubiquitinated proteins by the 26 S proteasome. *J. Biol. Chem.* **288**, 29215–29222 (2013).

Author contributions

R.S. and R.M. conceived and performed the study and wrote the manuscript.

Competing interests

The authors declare no competing interests.

Additional information

Extended data is available for this paper at https://doi.org/10.1038/s41591-020-01182-9.

Supplementary information is available for this paper at https://doi.org/10.1038/s41591-020-01182-9.

Correspondence and requests for materials should be addressed to R.M.

Peer review information Joao Monteiro was the primary editor on this article and managed its editorial process and peer review in collaboration with the rest of the editorial team.

Reprints and permissions information is available at www.nature.com/reprints.
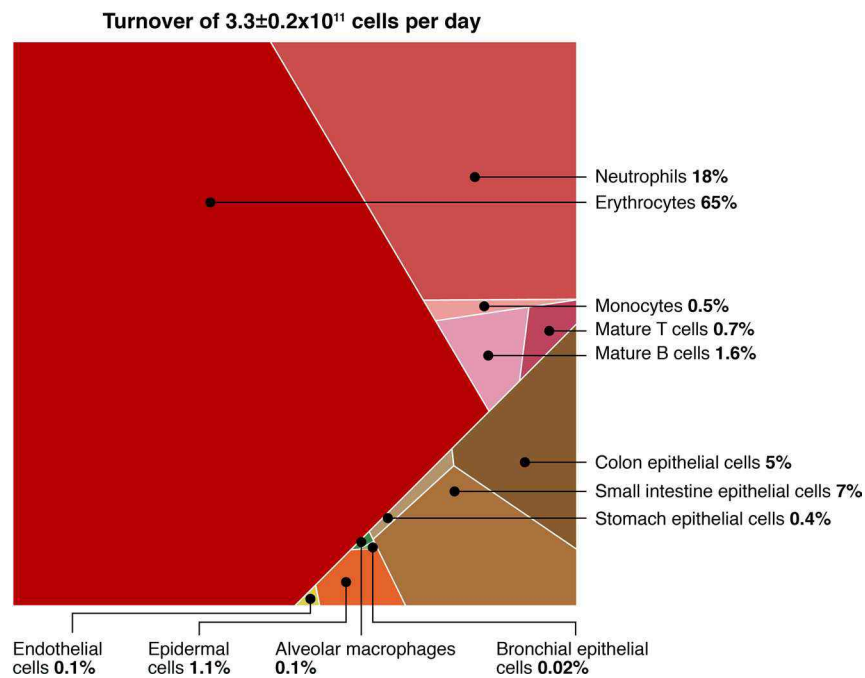
Extended Data Fig. 1 | Detailed distribution of the cellular turnover rate of human cells by cell type. To clarify the presentation, Fig. 1 and Fig. 2 in the manuscript body text only refer to the major groups of cells, presenting only the large contributions to the total turnover. This figure gives the same distribution but at a higher resolution, in which groups such as gastrointestinal cells, lymphocytes and lung cells are divided into their subpopulations. Polygon areas represent the fraction of total daily cell replacement for which the cell category accounts. Visualization performed using the online tool at http://bionic-vis.biologie.uni-greifswald.de/.

Total mass turnover rate of 80±20 grams per day
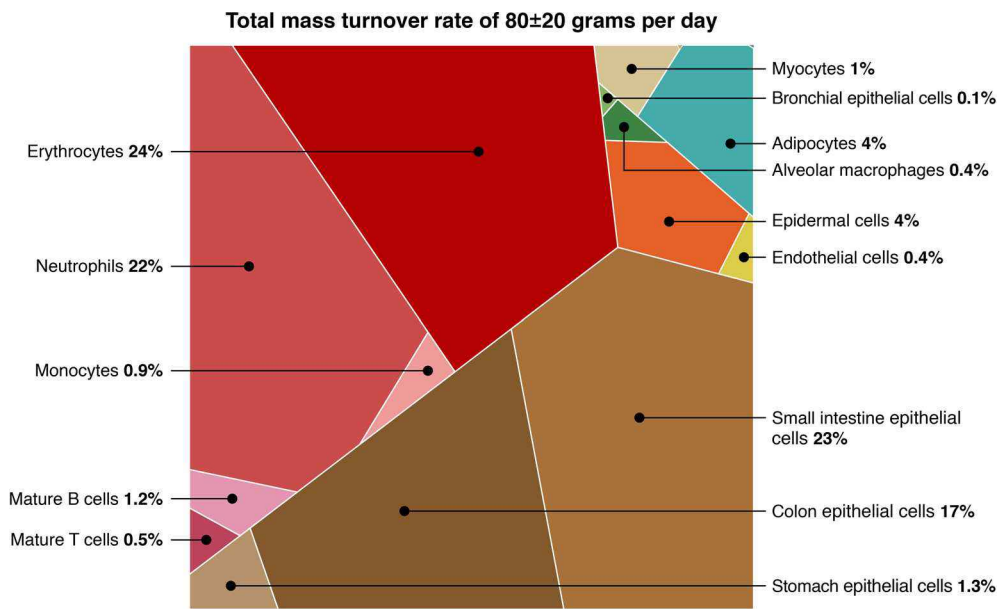
Extended Data Fig. 2 | Detailed distribution of cellular mass turnover rates of human cells by cell type. Presentation of the cellular mass turnover rates of human cells at higher resolution that in Fig. 2, which describes only the three largest groups of cell types (gastrointestinal cells, lymphocytes, and lung cells) from Fig. 2. are divided into their subpopulation. Polygon areas represent the fraction of total daily cell replacement for which the cell category accounts.
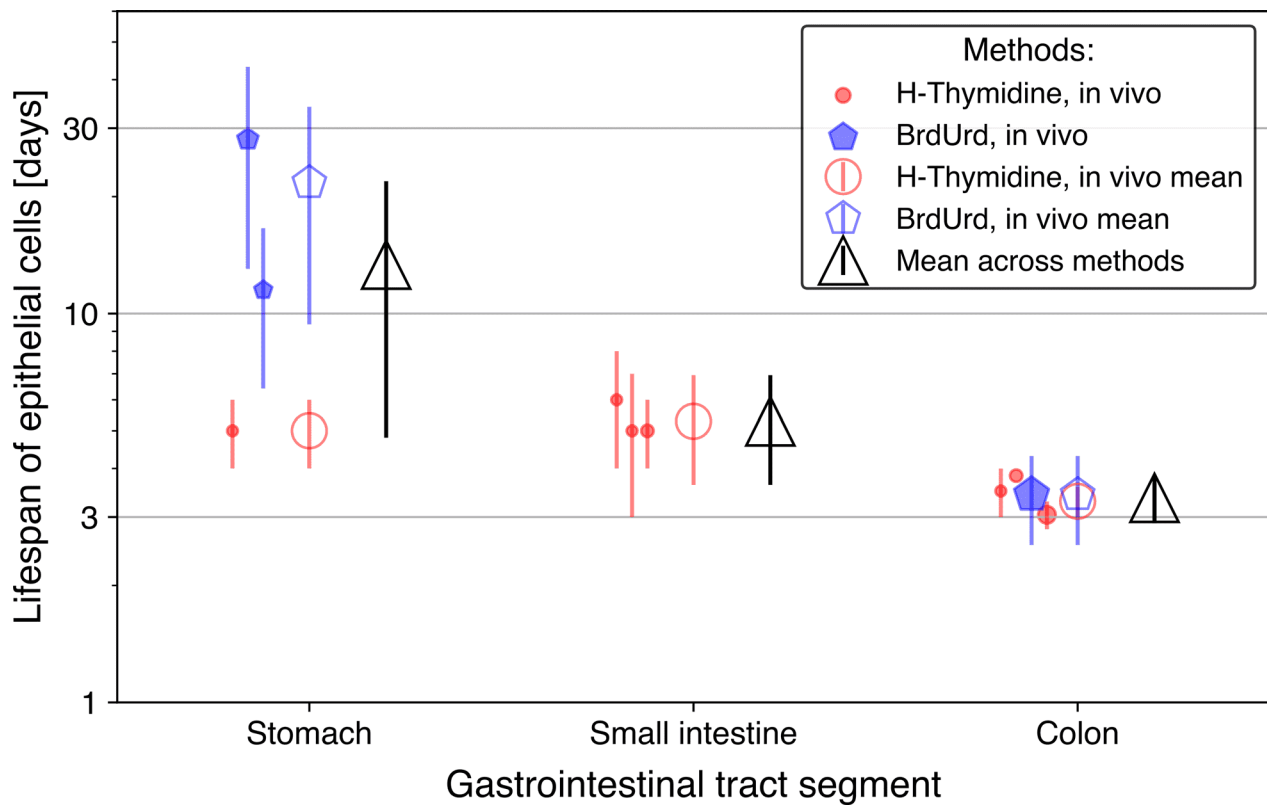
Extended Data Fig. 3 | Distribution of lifespan measurements of epithelial cells in the different segments of the gastrointestinal tract (GIT). For each segment (that is, stomach, small intestine, colon), the mean values and standard deviation from the different sources are presented on the left. The size of the point represents the number of measurements. In the middle, the mean values of each method are presented with error bars denoting 1 standard error. On the right-hand side, the overall mean value is shown with its standard error estimate.
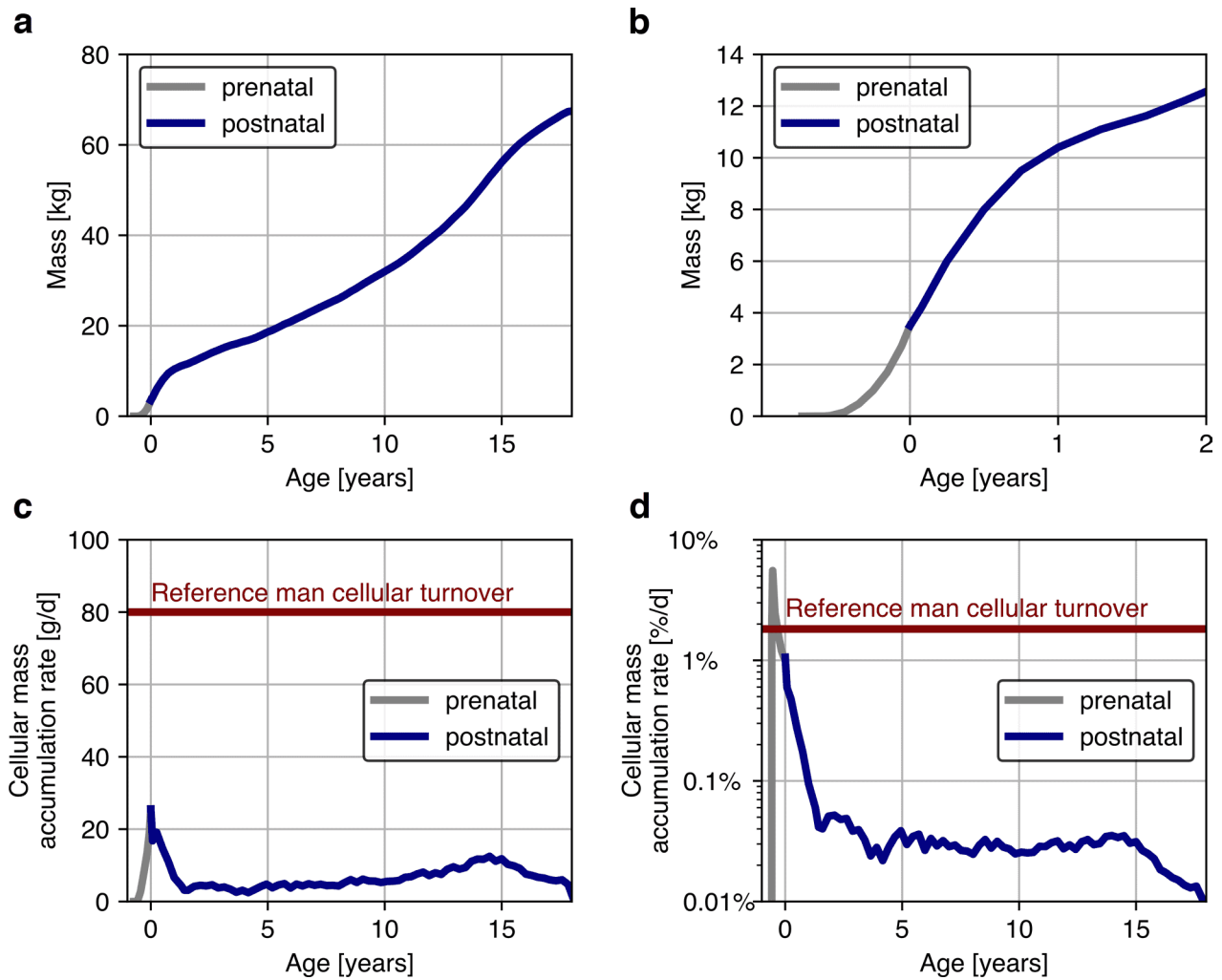
Extended Data Fig. 4 | Cellular mass accumulation rate during development. a. Mean mass of a human male from gestation through 18 years. Data taken from ICRP,2002. Grey line represents the gestation period. Blue line represents the postnatal period. **b**. Magnification of the early years of development, including gestation. **c**. The rate of mass accumulation calculated from the derivation of the cellular mass by time (derived from total mass assuming cellular mass represent a constant fraction of two third of total mass). Units were converted to grams per day. The mean cellular mass turnover rate in adult man homeostasis is given as reference. **d**. The rate of mass accumulation calculated from the derivation of the mass by time normalized to the total mass. The Y-axis is given in logarithmic scale. The mean cellular mass turnover rate in homeostasis as the percentage of the total weight of an adult man is given as reference.

Corresponding author(s):	Ron Milo
Last updated by author(s):	Nov 5, 2020

Reporting Summary

Nature Research wishes to improve the reproducibility of the work that we publish. This form provides structure for consistency and transparency in reporting. For further information on Nature Research policies, see our Editorial Policies and the Editorial Policy Checklist.

Statistics

For all statistical analyses, confirm that the following items are present in the figure legend, table legend, main text, or Methods section.

n/a	Confirmed	
☐	☒	The exact sample size (*n*) for each experimental group/condition, given as a discrete number and unit of measurement
☐	☒	A statement on whether measurements were taken from distinct samples or whether the same sample was measured repeatedly
☒	☐	The statistical test(s) used AND whether they are one- or two-sided *Only common tests should be described solely by name; describe more complex techniques in the Methods section.*
☒	☐	A description of all covariates tested
☒	☐	A description of any assumptions or corrections, such as tests of normality and adjustment for multiple comparisons
☐	☒	A full description of the statistical parameters including central tendency (e.g. means) or other basic estimates (e.g. regression coefficient) AND variation (e.g. standard deviation) or associated estimates of uncertainty (e.g. confidence intervals)
☒	☐	For null hypothesis testing, the test statistic (e.g. *F*, *t*, *r*) with confidence intervals, effect sizes, degrees of freedom and *P* value noted *Give P values as exact values whenever suitable.*
☒	☐	For Bayesian analysis, information on the choice of priors and Markov chain Monte Carlo settings
☒	☐	For hierarchical and complex designs, identification of the appropriate level for tests and full reporting of outcomes
☒	☐	Estimates of effect sizes (e.g. Cohen's *d*, Pearson's *r*), indicating how they were calculated

Our web collection on statistics for biologists contains articles on many of the points above.

Software and code

Policy information about availability of computer code

Data collection	Data was collected using Microsoft excel program (Microsoft Excel 2016 MSO (16.0.4738.1000) 32 bit) and python code (python version 3.7.9) given in Jupyter notebooks at the GitHub repository: https://github.com/milo-lab/cellular_turnover
Data analysis	All relevant code for analysis is given in the Jupyter Notebooks in the GitHub repository: https://github.com/milo-lab/cellular_turnover

For manuscripts utilizing custom algorithms or software that are central to the research but not yet described in published literature, software must be made available to editors and reviewers. We strongly encourage code deposition in a community repository (e.g. GitHub). See the Nature Research guidelines for submitting code & software for further information.

Data

Policy information about availability of data

All manuscripts must include a data availability statement. This statement should provide the following information, where applicable:

- Accession codes, unique identifiers, or web links for publicly available datasets
- A list of figures that have associated raw data
- A description of any restrictions on data availability

To generate our estimates of cellular turnover, we extracted values from the literature as detailed in the attached spreadsheet files. Our analysis pipeline is comprised of about 15 different Jupyter notebooks, which use the data extracted from the literature as input for generating our estimates. The data extracted for the purpose of our analysis, as well as the results of our analysis are summarized in tables available in the github repository located at https://github.com/milo-lab/cellular_turnover

Field-specific reporting

Please select the one below that is the best fit for your research. If you are not sure, read the appropriate sections before making your selection.

☒ Life sciences   ☐ Behavioural & social sciences   ☐ Ecological, evolutionary & environmental sciences

For a reference copy of the document with all sections, see nature.com/documents/nr-reporting-summary-flat.pdf

Life sciences study design

All studies must disclose on these points even when the disclosure is negative.

Sample size	Data on the abundance and lifespan of different cell types were collected by searching for relevant studies in the literature and manueling extracting published measurements.
Data exclusions	No data were excluded
Replication	No experiments in study
Randomization	No experiments in study
Blinding	No experiments in study

Reporting for specific materials, systems and methods

We require information from authors about some types of materials, experimental systems and methods used in many studies. Here, indicate whether each material, system or method listed is relevant to your study. If you are not sure if a list item applies to your research, read the appropriate section before selecting a response.

Materials & experimental systems

n/a	Involved in the study
☒	☐ Antibodies
☒	☐ Eukaryotic cell lines
☒	☐ Palaeontology and archaeology
☒	☐ Animals and other organisms
☒	☐ Human research participants
☒	☐ Clinical data
☒	☐ Dual use research of concern

Methods

n/a	Involved in the study
☒	☐ ChIP-seq
☒	☐ Flow cytometry
☒	☐ MRI-based neuroimaging